

**HIGH RESOLUTION  $^{26}\text{Al}$ - $^{26}\text{Mg}$  CHRONOMETRY OF CAIs FROM THE ALLENDE METEORITE** S. B. Jacobsen, R. Chakrabarti, M.C. Ranen and M. I. Petaev, Department of Earth and Planetary Sciences, Harvard University, 20 Oxford St. Cambridge, MA 02138, USA (jacobsen@neodymium.harvard.edu).

**Introduction:** Most evidence for the presence of  $^{26}\text{Al}$  ( $\tau_{1/2} = 0.73$  Ma) in the early Solar System comes from the study of CAIs, with most of them apparently having an initial  $^{26}\text{Al}/^{27}\text{Al}$  of  $\sim 5 \times 10^{-5}$  [1-3]. The recent comparison of  $^{26}\text{Al}$ - $^{26}\text{Mg}$ ,  $^{53}\text{Mn}$ - $^{53}\text{Cr}$  and  $^{207}\text{Pb}$ - $^{206}\text{Pb}$  systems [4] seems to validate  $^{26}\text{Al}$  as a chronometer and suggests that  $^{26}\text{Al}$  was widely and uniformly distributed in the early Solar System and can be used as a fine-scale chronometer. This evidence suggests that (i)  $^{26}\text{Al}$  was injected from a nearby stellar source and homogenized within the solar nebula in a short time period compared to its half-life and (ii)  $^{26}\text{Al}$  must have been an important heat source for melting small planetesimals. The exact initial  $^{26}\text{Al}/^{27}\text{Al}$  value is debated, with estimates ranging from  $\sim 4.5$  to  $6.5 \times 10^{-5}$  [5-10].

The MC-ICPMS measurements provide the most precise data for the Al-Mg system. [5-7] suggested that most CAIs formed within an extremely short time interval of  $\sim 20,000$  years. However, two research groups have obtained similarly precise isochrons for CAIs, but with quite different inferred initial  $^{26}\text{Al}/^{27}\text{Al}$  values of  $5.8 \times 10^{-5}$  and  $4.9 \times 10^{-5}$  [7,8]. The cause of this discrepancy may be due to: sample selection, interlaboratory calibration problems, or differences in data reduction procedures. We have initiated a study of  $^{26}\text{Al}$ - $^{26}\text{Mg}$  isotope systematics of well characterized CAIs by MC-ICPMS techniques aiming to resolve these problems and, in particular, to learn whether most CAIs formed over a very short time interval or not.

**Sample description:** We selected one very large ( $\sim 6.34$  grams) potato-shaped CAI (SJ101) and several smaller CAIs (SJ102 and SJ103) from the Allende CV3 meteorite. To obtain a representative “whole rock sample” of SJ101, the middle section (2.11 grams) was crushed to a fine powder, with one side of the CAI being used for a detailed petrologic and chemical study. This forsterite(Fo)-bearing (FoB) CAI is described in detail [11]. It is dominated by an Al-rich spinel(Sp)-clinopyroxene(Cpx) lithology which forms rather large, contorted islands separated by sinuous bands and/or pockets of a Fo-Cpx lithology. The inclusion lacks the Al-enriched mantle typical of other FoBs. There is no ‘classic’ Wark-Lovering (WL) rim. Instead, the peripheral portions of SJ101 contain rather large, discontinuous anhedral masses of Sp in a reaction relationship with the  $\text{Al}_2\text{O}_3$ -poor and  $\text{SiO}_2$ -rich (up to 55 wt.%) Cpx which, in many cases, is in direct contact with the Allende matrix. No perovskite or hibonite was found in these Sp masses so far. The inclusion

contains cavities and was cross-cut by several more or less straight cracks extended to its very periphery. Both the Sp-Cpx and Fo-Cpx lithologies display igneous textures with Sp and Fo being poikilitically enclosed in clinopyroxene. A few grain boundaries observed in BSE images of the Sp-Cpx lithology suggests that the Cpx is polycrystalline and rather coarse-grained; this may also be the case of the Fo-Cpx lithology.

SJ102 is a small,  $\sim 0.5$  cm spherical Type B1 CAI. A 2 mg fragment was extracted for analysis, another small chip is used for petrologic studies. This Type B1 inclusion consists of  $\text{TiO}_2$ -rich Cpx, nearly pure Sp and zoned  $\text{Al}_2\text{O}_3$ -rich melilite with the MgO content decreasing outward from  $\sim 8$  wt% near the boundary with Cpx down to  $\sim 2$  wt% at the periphery of the inclusion. Melilite displays irregular patches of alteration products which mainly consist of grossular and, to a lesser extent, anorthite. Na is present, but in quite low concentrations. No classic WL rim was observed, but it may not be exposed. Several blobs of massive Sp associated with anorthite were observed in the top left corner of the inclusion. The pronounced compositional zoning in melilite points to an evaporative loss of Si and Mg during the formation of this CAI, consistent with the well-known models of formation of the Type B1 CAIs.

SJ103 is a small,  $\sim 1$  cm irregular Type B2 CAI. A 8 mg fragment was extracted for analysis, another small chip is used for petrologic studies. This Type B2 inclusion consists of low- $\text{TiO}_2$  Cpx, anorthite,  $\text{Al}_2\text{O}_3$ -rich melilite, and nearly pure Sp. The melilite and Cpx show only minor zoning. The ‘classic’ WL rim contains large anhedral masses of Sp and perovskite along with the small blades of Mg-bearing hibonite. Right underneath the WL rim there are rather thick Al-rich pockets which consist of fine intergrowths of Sp, anorthite, and an Al-rich phase with approximate formula  $(\text{Na,Ca})_2(\text{Mg,Fe,Al})\text{Al}_6\text{Si}_4\text{O}_{20}$ . Rare hibonite blades are also present in these pockets. The melilite separating such pockets contains anhedral  $\text{TiO}_2$ -bearing Sp grains as well as tiny perovskite crystals. It appears that the material underneath the WL rim has experienced variable degrees of evaporation probably not related to the formation of the WL rim.

**Analytical methods:** Our methods have been discussed earlier [12]. The radiogenic effect due to  $^{26}\text{Al}$  decay is represented in deviations in parts in  $10^4$  from the terrestrial Mg standard (DSM3) as  $\epsilon_{26\text{Mg}}$ , and can

be calculated from the measured  $\delta^{25}\text{Mg}$  and  $\delta^{26}\text{Mg}$  values:

$$\varepsilon_{26\text{Mg}} = \left\{ [1 + 10^{-3}\delta^{26}\text{Mg}][1 + 10^{-3}\delta^{25}\text{Mg}]^{-(1/\rho)} - 1 \right\} \times 10^4$$

where  $\rho$  is a fractionation coefficient that is, in general, not precisely known. In the exponential law commonly used for correcting for mass fractionation in TIMS measurements, the value of  $\rho$  is 0.51101 [for this law  $\rho = \ln(m_{25\text{Mg}}/m_{24\text{Mg}})/\ln(m_{26\text{Mg}}/m_{24\text{Mg}})$  and the  $m_{i\text{Mg}}$  are the masses for the Mg isotopes]. The raw  $^{25}\text{Mg}/^{24}\text{Mg}$  and  $^{26}\text{Mg}/^{24}\text{Mg}$  ratios measured with the IsoProbe-P yield a  $\rho$  value of  $\sim 0.52$  which is substantially higher than the exponential law value and close to the equilibrium value [13]. It is clear that the exponential law is not correcting properly for mass spectrometric fractionation in the IsoProbe-P. We use the "law" determined by data obtained with this instrument. This is effectively done by first using a sample-standard bracketing method to obtain  $\delta^{25}\text{Mg}$  and  $\delta^{26}\text{Mg}$  values then to apply a correction for non-instrumental (natural) mass fractionation to obtain a precise estimate of  $\varepsilon_{26\text{Mg}}$  (equation above).

**Results:** Our results for  $\delta^{25}\text{Mg}$  and  $\varepsilon_{26\text{Mg}}$  are plotted versus  $^{27}\text{Al}/^{24}\text{Mg}$  in Figures 1 and 2. For calculating  $\varepsilon_{26\text{Mg}}$  we used the exponential law coefficient to be able to compare our data directly with the results of [5] and [8]. All our data were reproduced on two instruments (both IsoProbe-P), with some of the data having been reproduced in both high ( $\sim 3000$ ) and low mass resolution ( $\sim 500$ ). Our data when plotted in the fossil isochron diagram are consistent with [5,8], but not with [6,7]. We find no evidence for supracanonical  $^{26}\text{Al}/^{27}\text{Al}$  ratios in CAIs. Most CAIs appear to have formed within a very short time interval (20 – 40,000 years).

Since there is some ambiguity of what  $\rho$  value should be used for CAIs that have experienced substantial Mg isotopic fractionation from the average Solar System value there is still some uncertainty in the slope of the array in Figure 2. One of our goals is to determine the  $\rho$  value by analyzing CAIs with a large range of Mg isotope fractionations, rather than relying on the exponential law. More data on CAIs are needed to obtain a  $\rho$ -value that applies to evaporation of CAIs. Based on evaporation experiments an experimentally determined value of  $\rho = 0.514$  was recommended by Davis et al. [14]. We are also conducting TIMS measurements of Mg isotopes to determine if evaporation during thermal ionization is closer to the exponential law ( $\rho = 0.511$ ) or the Rayleigh fractionation law ( $\rho = 0.516$ ).

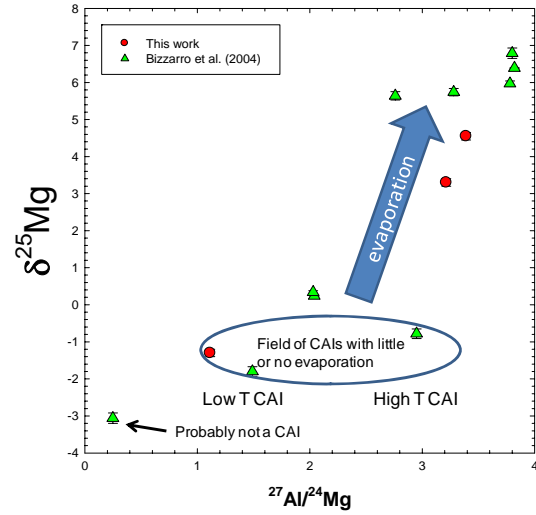


Figure 1.

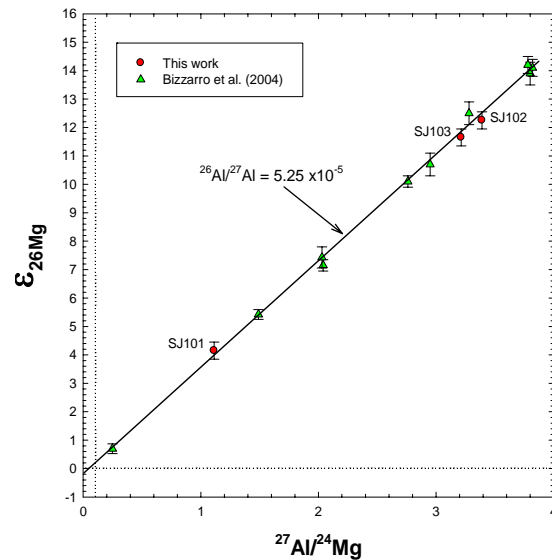


Figure 2.

**References:** [1] Lee T. et al. (1977) *ApJ*, 211, L107-L110. [2] Macpherson et al. (1995) *Meteoritics* 30, 365-386. [3] Hsu W. et al. (2000) *EPSL*, 182, 15-29. [4] Kita N. T. et al. (2005) *ASP Conference Series*, 341, pp.558-587. [5] Bizzarro M. et al. (2004) *Nature*, 431, 275-278. [6] Bizzarro M. et al. (2005) *Nature*, 435, 1280. [7] Thrane K. et al. (2006) *ApJ*, 646, L159-L162. [8] Jacobsen B. et al. (2007) *LPS*, XXXVIII, 1491. [9] Young E.D. et al. (2005) *Science*, 308, 223-227. [10] Cosarinsky M. et al. (2006) *LPS*, 37, 2357. [11] Petaev M.I. & Jacobsen S.B. (2007) *CMES Workshop 2007 Kauai*, p.82-83. [12] Jacobsen S.B. et al. (2007) *CMES Workshop 2007 Kauai*, p.82-83. [13] Young E.D. & Galy A. (2004) *Reviews in mineralogy and geochemistry*, 55, 197-230. [14] Davis A.M. et al. (2005) *LPS*, 36, 2334.